Inorganic Chemistry

Article

pubs.acs.org/IC

Ruthenium Hydrides Containing the Superhindered Polydentate Polyphosphine Ligand $P(CH_2CH_2P^tBu_2)_3$

Ryan Gilbert-Wilson, [†] Leslie D. Field,*[,†] and Mohan Bhadbhade[‡]

[†]School of Chemistry, The University of New South Wales, Sydney, NSW 2052, Australia

[‡]Mark Wainwright Analytical Centre, The University of New South Wales, Sydney, NSW 2052, Australia

Supporting Information

ABSTRACT: The complex $RuH_2(N_2)(P^2P_3^{tBu})$ (**1**) containing the extremely bulky PP_3-type ligand $P^2P_3^{tBu} = P(CH_2CH_2P^tBu_2)_3$ was synthesized by reduction of $RuCl_2(P^2P_3^{tBu})$ (**2**) with Na/NH_3 under a N_2 atmosphere. Like other complexes containing the $P^2P_3^{tBu}$ ligand, only three of the four donor phosphines are coordinated, and one of the phosphines remains as a dangling pendant phosphine. Reduction of $RuCl_2(P^2P_3^{tBu})$ (**2**) with a range of the more usual hydride reducing agents afforded the previously unknown ruthenium hydride complexes $RuHCl(P^2P_3^{tBu})$ (**3**), $RuH(BH_4)(P^2P_3^{tBu})$ (**6**), $RuH(AlH_4)(P^2P_3^{tBu})$ (**7**), and the ruthenium(II) trihydride $K[Ru(H)_3(P^2P_3^{tBu})]$ (**8**). The ruthenium tetrahydride containing a coordinated H_2 ligand $RuH_2(H_2)(P^2P_3^{tBu})$ (**10**) was synthesized by exchange of N_2 in **1** by H_2. Complexes **1**, **3**, **6**, **7**, and **8** were characterized by crystallography and multinuclear NMR spectroscopy.

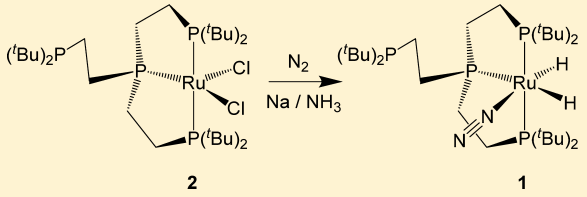

2 1

INTRODUCTION

It was a ruthenium dinitrogen complex, $[Ru(NH_3)_5(N_2)]^{2+}$, in 1965[1] which originally sparked the study of dinitrogen as a transition metal ligand, and since then a wealth of transition metal dinitrogen complexes have been successfully synthesized.[2] A common feature of the complexes with the most interesting reaction chemistry is that they usually contain a sterically hindered ligand environment around the metal, which protects and stabilizes the reactive metal center.[3]

We have extensively studied metal hydrido and dihydrido dinitrogen complexes where there are both hydrido and N_2 substituents bound to the same metal center. Interest in the chemistry of dinitrogen hydride complexes has been driven by the discovery that iron hydrides are probably some of the key intermediates in the nitrogen fixation mechanism used by the enzyme nitrogenase,[4] and metal dinitrogen hydrides are likely intermediates in any transition metal mediated reduction of dinitrogen.

There are now a number of complexes of iron and ruthenium where both hydrido and dinitrogen ligands are bound at the same metal center. In this study, we have investigated complexes with the sterically hindered PP_3 ligand = $P(CH_2CH_2P^tBu_2)_3$ ($P^2P_3^{tBu}$). The polydentate polyphosphine ligands $P(CH_2CH_2PR_2)_3$ (PP_3) are known with phenyl-,[5] methyl-,[6] isopropyl-,[7] *tert*-butyl-,[8] and cyclohexyl-[9] substituents on the terminal phosphine donors. The PP_3-type ligands generally bind strongly through all four donors with Fe and Ru halides, with the dinitrogen complexes accessible through reduction under a nitrogen atmosphere.[6b,7,10] $P^2P_3^{tBu}$ is arguably the most sterically hindered of the known PP_3-type ligands.

Much of the chemistry around metal complexes containing coordinated dinitrogen has focused on activating the coordinated N_2 and driving reactions at N_2. The chemistry is often complicated by competing pathways, and in many instances, reaction at the metal center is more facile than on N_2. Furthermore, if the reaction conditions contain reagents that are themselves good ligands, then substitution of the weakly coordinated N_2 is always possible. We have been exploring iron and ruthenium complexes with PP_3-type ligands with very bulky substituents in an attempt to slow reactions at the metal center and promote reactions at the coordinated N_2.

This paper describes approaches to the synthesis of the complex $RuH_2(N_2)(P^2P_3^{tBu})$ (**1**, Scheme 1). For this target, the starting material was the complex $RuCl_2(P^2P_3^{tBu})$ (**2**) which was reported in 2012[11] and in $RuCl_2(P^2P_3^{tBu})$, only three of the four donor phosphines are coordinated with one of the phosphine donors remaining as a dangling pendant ligand.

Scheme 1

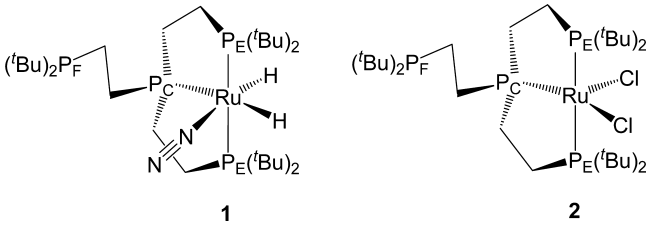

1 2

Received: August 6, 2014
Published: November 12, 2014

Scheme 2

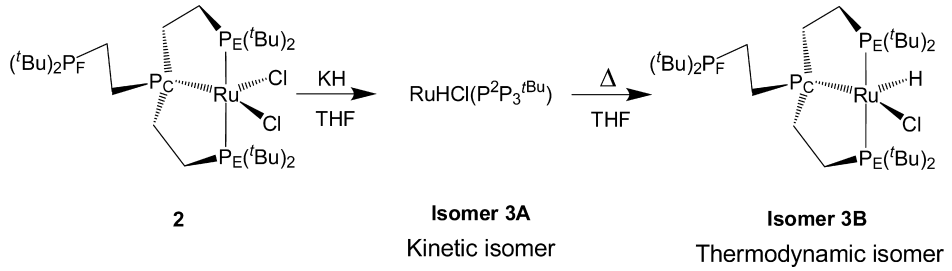

2 **Isomer 3A** Kinetic isomer **Isomer 3B** Thermodynamic isomer

RESULTS AND DISCUSSION

The specific target complex for this program was $RuH_2(N_2)$-$(P^2P_3^{tBu})$ (**1**), and the approach was to substitute the two chloro ligands of the known complex $RuCl_2(P^2P_3^{tBu})$ (**2**) with two hydride ligands.

A number of more conventional hydridic reducing reagents were investigated in an attempt to achieve the conversion of **2** → **1**, yielding a range of new ruthenium hydride complexes.

$RuHCl(P^2P_3^{tBu})$ (3). Stirring a suspension of $RuCl_2(P^2P_3^{tBu})$ (**2**) and potassium hydride in THF at room temperature afforded two different species by NMR spectroscopy. Each species has three $^{31}P\{^1H\}$ resonances and a single metal hydride resonance in the ^1H spectrum located near −30 ppm. The two species show similar $^{31}P\{^1H\}$ and ^1H NMR spectra with the same coupling patterns between the respective peaks for each complex, indicating that they are probably isomers.

After the initial reaction, the complex with the more shielded ^1H hydride (δ −30.61) resonance was in excess (isomer A). Over time, the proportion of this complex decreased while there was a corresponding increase of the second complex with a slightly less shielded ^1H hydride resonance (δ −30.47; isomer B). The conversion process was accelerated by heating.

These complexes are probably kinetic (isomer A) and thermodynamic (Isomer B) isomers of $RuHCl(P^2P_3^{tBu})$ (**3**). Heating of the reaction mixture at 60 °C for 6 h resulted in full conversion to isomer B (Scheme 2). As there are very small changes in the ^1H and ^{31}P NMR spectra of isomer A and isomer B, it is assumed that there are only a minor geometric differences between isomer A and isomer B. Reduction of $RuCl_2(P^2P_3^{tBu})$ with an excess of $SiEt_3H$ also gave $RuHCl$-$(P^2P_3^{tBu})$ (**3**), predominantly as isomer B.

Crystals of the thermodynamic isomer (isomer **3B**) suitable for structural analysis were grown by evaporation of a 1:1 THF/toluene solution of complex **3B** (Figure 1) with selected bond angles and lengths given in Table 1.

The geometry of $RuHCl(P^2P_3^{tBu})$ (**3**) is an extremely distorted square-based pyramid, with the three phosphine donors and the chloro ligand forming the base of the pyramid and the hydrido ligand at the apex. The geometric parameter indicative of five-coordinate complex geometry τ was found to be 0.14 (τ = 0 corresponds to perfect square pyramidal geometry, and τ = 1 is perfect trigonal-bipyramidal geometry).[12] The significant distortion comes from the large difference in apex to base bond angles between the extremely tight P2−Ru1−H1 bond angle of 72(2) in contrast to the wide Cl1−Ru1−H1 angle of 134(2), which are on opposite sides of the pyramid. The location of hydrides in X-ray crystallography is not always precise, so it is difficult to draw conclusions from this irregular geometry.

The three other reported structures of five-coordinate ruthenium hydrido chloro complexes with three phosphine donors are RuHCl(R,R-1,2-bis(diphenylphosphinamino)-cyclohexane)(PPh_3),[13] RuHCl(bis(phosphaadamantyl)-propane)(PPh_3),[14] and RuHCl(PCy_3)(Fe(η^5-$C_5H_4PPh_2$)$_2$).[15] All of these complexes share a similarity in that they possess sterically bulky phosphine donors which prevent the coordination of a fourth phosphine donor. This is consistent with the sterically bulky nature of $P^2P_3^{tBu}$, leading to the formation of $RuHCl(P^2P_3^{tBu})$ (**3**) as a five-coordinate complex. Complex **3** has considerably different geometry than the other listed compounds of this type. While the other hydrido chloro complexes are also distorted square pyramids, they have a phosphine donor located at the apex and hydrido and chloro ligands *trans* to each other in the base of the pyramid.

The $^{31}P\{^1H\}$ NMR spectrum of $RuHCl(P^2P_3^{tBu})$ (**3**) shows the central phosphine P_C as a doublet of triplets at 120.8 ppm coupled to the pendant terminal phosphine P_F and both of the bound terminal phosphines P_E. The signal for P_E is a doublet at 86.4 ppm with $^2J_{PE-PC}$ = 14 Hz, and the signal for P_F is a

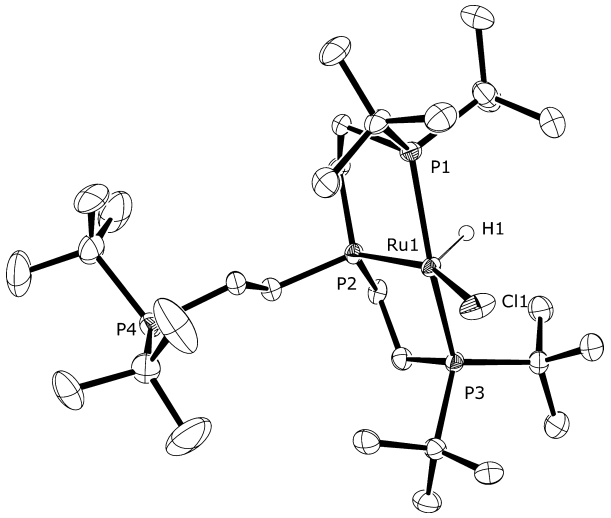

Figure 1. ORTEP plot (50% thermal ellipsoids) of $RuHCl(P^2P_3^{tBu})$ (**3**), within each asymmetric unit. Selected hydrogen atoms have been omitted for clarity.

Table 1. Selected Bond Lengths (Å) and Bond Angles (deg) for $RuHCl(P^2P_3^{tBu})$ (3)

Ru1−Cl1	2.4488(13)	Ru1−H1	1.73(6)
Ru1−P1	2.3393(12)	Ru1−P2	2.1776(12)
Ru1−P3	2.3305(12)		
Cl1−Ru1−H1	134(2)	P1−Ru1−Cl1	97.93(4)
P2−Ru1−Cl1	153.45(5)	P3−Ru1−Cl1	97.95(4)
P1−Ru1−H1	84(2)	P2−Ru1−H1	72(2)
P3−Ru1−H1	79.2(19)	P1−Ru1−P2	85.41(4)
P1−Ru1−P3	161.96(5)	P2−Ru1−P3	84.22(4)

dx.doi.org/10.1021/ic501895s | *Inorg. Chem.* 2014, 53, 12469−12479

Scheme 3

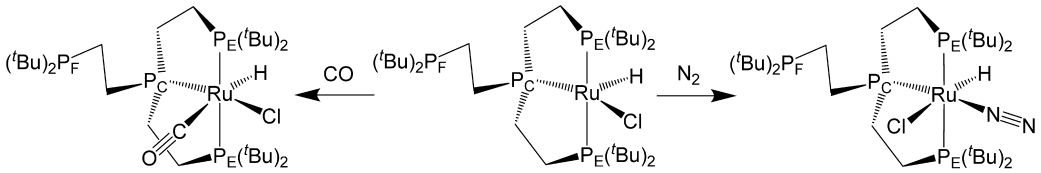

doublet at 33.7 ppm with $^{3}J_{PF-PC}$ = 30 Hz. The hydride resonance at −30.47 ppm is a doublet of triplets, with coupling to P_E and to P_C. The extremely high field shift of the hydride proton is consistent with a hydride location trans to a vacant site.

Even using an excess of potassium hydride in the reaction mixture, RuHCl($P^2P_3^{tBu}$) (**3**) was the only hydride species formed under the reaction conditions, and there was no evidence for the substitution of the second chloride.

While **3** is a stable but highly hindered species, it is coordinatively unsaturated and reacts with small molecule donors to form new complexes (Scheme 3). Reaction of RuHCl($P^2P_3^{tBu}$) (**3**) with carbon monoxide afforded RuHCl(CO)($P^2P_3^{tBu}$) (**4**) as a beige powder, and crystals suitable for structural analysis were grown by slow evaporation of a toluene solution. Slow evaporation of a toluene/hexane solution of RuHCl($P^2P_3^{tBu}$) (**3**) under an atmosphere of N_2 over an extended period of time deposited crystals of RuHCl(N_2)($P^2P_3^{tBu}$) (**5**) suitable for structural analysis. Characterization and molecular structures for RuHCl(CO)($P^2P_3^{tBu}$) (**4**) and RuHCl(N_2)($P^2P_3^{tBu}$) (**5**) are contained in the Supporting Information.

RuH(BH_4)($P^2P_3^{tBu}$) (6). Treatment of $RuCl_2$($P^2P_3^{tBu}$) (**2**) with sodium borohydride in methanol resulted in the precipitation of a yellow solid. Isolation of the solid by filtration afforded the hydrido borohydride complex RuH(μ^2-BH_4)($P^2P_3^{tBu}$) (**6**; Scheme 4). Crystals suitable for structural analysis were grown by evaporation of a toluene solution of **6** (Figure 2) with selected bond angles and lengths given in Table 2.

Scheme 4

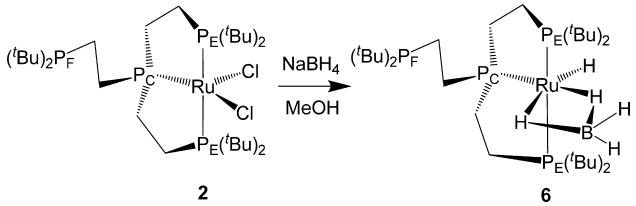

The geometry of RuH(BH_4)($P^2P_3^{tBu}$) (**6**) is that of a distorted octahedron with the three phosphine donors binding in a meridional arrangement around the ruthenium center. The remaining three coordination sites are occupied by a hydride and two bridging hydrides of a tetrahydridoborate ligand.

The three coordinated phosphine donors define a plane in the structure, and the hydrido and BH_4 ligands are located on either side of the PPP plane. The hydride ligand occupies the more hindered face of the molecule with the BH_4 located on the less hindered face. The structure of RuH(BH_4)($P^2P_3^{tBu}$) (**6**) is analogous to that of RuH(BH_4)(PMe_3)$_3$,[16] which has the same donor atoms and geometry and only varies in the nature

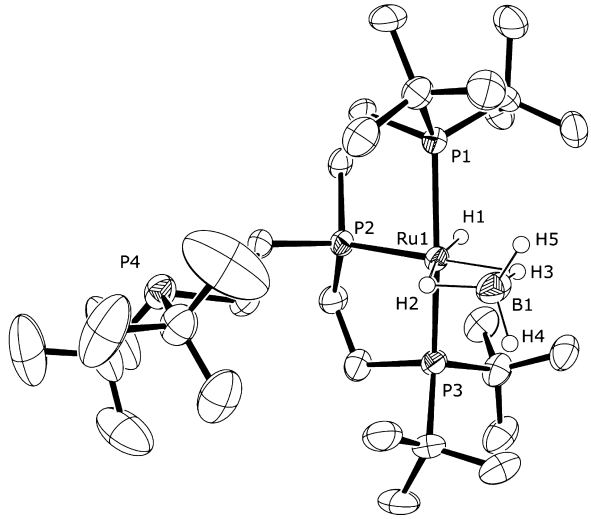

Figure 2. ORTEP plot (50% thermal ellipsoids) of RuH(BH_4)($P^2P_3^{tBu}$) (**6**), within each asymmetric unit. Selected hydrogen atoms have been omitted for clarity.

Table 2. Selected Bond Lengths (Å) and Angles (deg) for RuH(BH_4)($P^2P_3^{tBu}$) (6)

Ru1−B1	2.281(8)	Ru1−H1	1.55(5)
Ru1−H2	1.99(5)	Ru1−H3	1.79(5)
Ru1−P1	2.3467(17)	Ru1−P2	2.2118(15)
Ru1−P3	2.3474(17)		
H1−Ru1−H2	166(2)	H1−Ru1−H3	100(3)
H2−Ru1−H3	66(2)	P1−Ru1−P2	83.69(6)
P1−Ru1−P3	160.00(6)	P2−Ru1−P3	84.64(6)
P1−Ru1−H1	79.0(19)	P1−Ru1−H2	98.2(14)
P1−Ru1−H3	95.9(17)	P2−Ru1−H1	79.7(18)
P2−Ru1−H2	113.9(15)	P2−Ru1−H3	179.6(18)
P3−Ru1−H1	79.0(19)	P3−Ru1−H2	101.4(14)
P3−Ru1−H3	95.8(17)		

of the phosphine donors. The ruthenium hydride bond distance in the two structures are comparable with a value of 1.55(5) Å for **6** compared to 1.49(4) Å for RuH(BH_4)(PMe_3)$_3$. Other differences between the structures can be attributed to the different steric environment produced by the bulky $P^2P_3^{tBu}$ ligand when compared to the less bulky PMe_3 ligands.

The $^{31}P\{^{1}H\}$ NMR spectrum of RuH(BH_4)($P^2P_3^{tBu}$) (**6**) displays three distinct resonances, a doublet of triplets at 118.5 ppm, a doublet at 97.7 ppm, and a doublet at 35.5 ppm. These correspond to the central phosphine P_C, the two bound terminal phosphines P_E, and the free phosphine P_F, respectively. The ^{1}H NMR spectrum of RuH(BH_4)($P^2P_3^{tBu}$) (**6**) displays alkyl ligand resonances as well as resonances assigned to the various hydride ligands. The signal for the ruthenium hydride H_A (−19.18 ppm) is a doublet of triplets

dx.doi.org/10.1021/ic501895s | Inorg. Chem. 2014, 53, 12469−12479

due to coupling to the coordinated phosphine donors. The tetrahydridoborate hydride resonances consist of a broad two-proton resonance at 5.29 ppm corresponding to the terminal hydrides and a second broad two-proton resonance at −6.26 ppm for the bridging hydrides (Figure 3A). The ^{1}H resonances of the borohydride protons are broadened by exchange, but at a lower temperature, the resonances of the ruthenium-bound bridging hydrides are resolved.

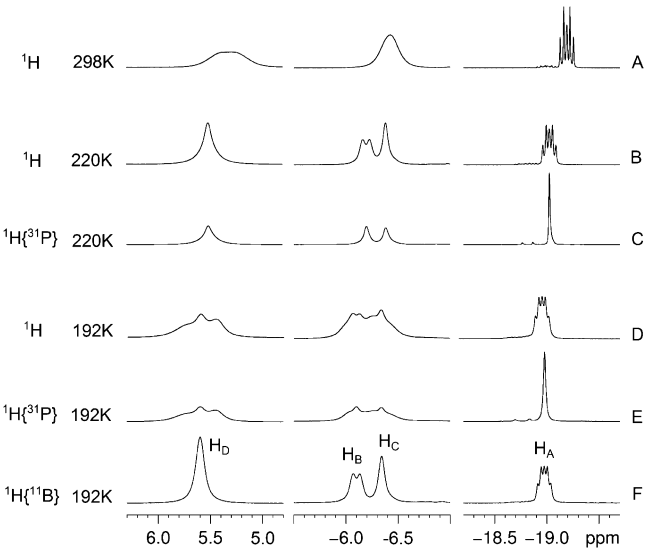

Figure 3. Hydride region of RuH(BH$_4$)(P^{2}P$_3^{tBu}$) (**6**; 600 MHz, toluene-d_8 solvent). (A) ^{1}H NMR spectrum at 298 K; (B) ^{1}H NMR spectrum at 220 K; (C) ^{1}H{^{31}P} NMR spectrum at 220 K; (D) ^{1}H NMR spectrum at 192 K; (E) ^{1}H{^{31}P} NMR spectrum at 192 K; (F) ^{1}H{^{11}B} NMR spectrum 192 K.

Low temperature ^{1}H and ^{1}H{^{31}P} NMR spectra of RuH(BH$_4$)(P^{2}P$_3^{tBu}$) (**6**) enable further resolution of the bridging dihydride resonances (Figure 3, Scheme 5). When

Scheme 5

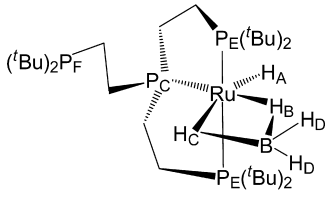

6

the temperature was decreased to 220 K, the two equivalent terminal hydrides of the borohydride (H_D) appear as a single resonance at 5.52 ppm, but the two bridging hydrides resolve into two separate resonances, a doublet at −6.19 ppm (corresponding to the bridging hydride H_B) with a coupling constant of $^2J_{H-P}$ = 40 Hz to P_C and a broadened singlet at −6.38 ppm, corresponding to H_C (Figure 3B and C). At 192 K, in ^{1}H and ^{1}H{^{31}P} NMR spectra the signals for hydrides (H_D) and the bridging hydrides (H_B and H_C) all show an unsymmetrical broadening resulting from coupling to boron at this low temperature, and decoupling ^{11}B substantially removes the broadening at 192 K (Figure 3F).

RuH(BH$_4$)(P^{2}P$_3^{tBu}$) (**6**) is stable over time to a range of conditions including exposure to methanol and gentle heating. The summarized NMR and structural analysis above for **6** is consistent with a monometallic complex in both solution and the solid state.

RuH(AlH$_4$)(P^{2}P$_3^{tBu}$) (7). Slow addition of a THF solution of LiAlH$_4$ to RuCl$_2$(P^{2}P$_3^{tBu}$) (**2**) in THF decolorized the solution and afforded the hydrido aluminumtetrahydride complex RuH(AlH$_4$)(P^{2}P$_3^{tBu}$) (**7**; Scheme 6). Crystals suitable for

Scheme 6

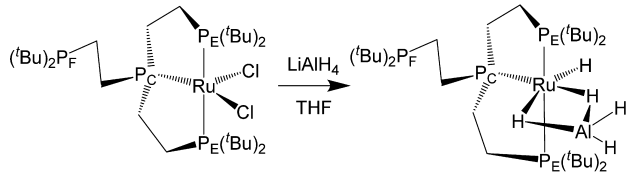

2 **7**

structural analysis were grown from a concentrated benzene-d_6 solution of **7** (Figure 4), and selected bond lengths and angles

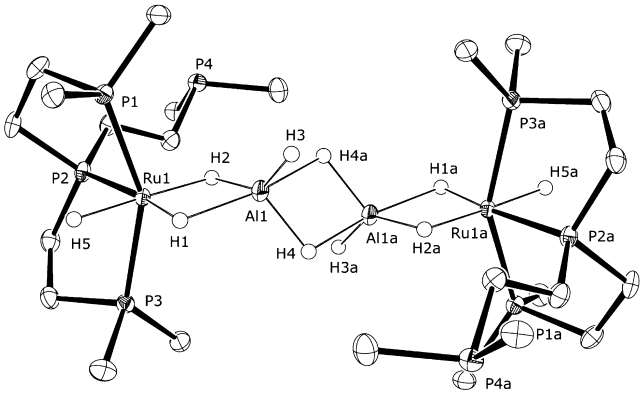

Figure 4. ORTEP plot (50% thermal ellipsoids) of RuH(AlH$_4$)(P^{2}P$_3^{tBu}$) (**7**), within each asymmetric unit. Selected hydrogen atoms and *tert*-butyl methyl groups of have been omitted for clarity.

are included in Table 3. This structure revealed that RuH(AlH$_4$)(P^{2}P$_3^{tBu}$) (**7**) exists as the dimer [RuH(AlH$_4$)(P^{2}P$_3^{tBu}$)]$_2$ in the solid state.

The geometry of RuH(AlH$_4$)(P^{2}P$_3^{tBu}$) (**7**) is that of a distorted octahedron around ruthenium with the three phosphine donors in a meridional arrangement. The three

Table 3. Selected Bond Lengths (Å) and Bond Angles (deg) for RuH(AlH$_4$)(P^{2}P$_3^{tBu}$) (7)

Ru −Al1	2.4702(6)	Ru1−H5	1.58(2)
Ru1−H1	1.66(2)	Ru1−H2	1.66(2)
Ru1−P1	2.3399(5)	Ru1−P2	2.2619(5)
Ru1−P3	2.3362(5)	Al1−H1	1.86(2)
Al1−H2	1.75(2)	Al1−H3	1.54(2)
Al1−H4	1.60(2)	Al1−H4a	1.86(2)
H1−Ru1−H2	93.4(10)	H1−Ru1−H5	87.1(10)
H2−Ru1−H5	177.9(9)	P1−Ru1−P2	83.980(18)
P1−Ru1−P3	151.612(19)	P2−Ru1−P3	84.658(19)
P1−Ru1−H1	94.2(7)	P1−Ru1−H2	103.1(7)
P1−Ru1−H5	78.9(7)	P2−Ru1−H1	171.8(7)
P2−Ru1−H2	94.8(7)	P2−Ru1−H5	84.8(7)
P3−Ru1−H1	93.4(7)	P3−Ru1−H2	103.7(7)
P3−Ru1−H5	74.2(7)		

dx.doi.org/10.1021/ic501895s | *Inorg. Chem.* 2014, 53, 12469−12479

other coordination sites are occupied by hydrides, two of which are part of the tetrahydridoaluminate ligand. The ruthenium centers are bridged through their tetrahydridoaluminate ligands, with H4 of each monomer bonding tightly to the aluminum (Al1a) of the other monomer with a bond distance of 1.86 Å. This is the first structure of a ruthenium complex with a coordinated tetrahydridoaluminate ligand, dimerized or otherwise. The structure of the binuclear ruthenium species $Cp^*_2Ru_2(\mu\text{-}Ph_2PCH_2PPh_2)(\mu\text{-}AlH_5)$[17] in which an AlH_5^{2-} fragment bridges two ruthenium(II) centers has been reported, although the usefulness of this structure for structural comparison is limited, due to the single aluminate nature of the bridge. The complexes $[Cp^*_2ZrH(\mu2\text{-}H_2AlH_2)]_2$[18] and $[(dmpe)_2MnH_2AlH_2]_2$[19] contain the same dimerized tetrahydridoaluminate bridge between two metal centers as **7**, and these hydridoaluminate bridges share similar bond lengths and geometries to that observed for the structure of **7**.

In the $^{31}P\{^1H\}$ NMR spectrum of $RuH(AlH_4)(P^2P_3{}^{tBu})$ (**7**), the resonance for the bound terminal phosphines P_E is observed as a doublet at 113.5 ppm, the central phosphine P_C resonance as a doublet of triplets at 111.7 ppm, and the dangling pendant terminal phosphine P_F resonance as a doublet at 35.1 ppm. In the ^1H NMR spectrum of $RuH(AlH_4)(P^2P_3{}^{tBu})$ (**7**), a doublet of triplets of doublets (due to $^2J_{H-P}$ and $^2J_{H-H}$ coupling) located at −13.54 ppm is assigned to the nonbridging ruthenium hydride. Three distinct resonances assigned to the hydrides of the tetrahydridoaluminate ligand were also observed in the ^1H NMR spectrum. The broad resonance at 2.81 ppm was assigned to the hydrides attached solely to aluminum while the doublet of triplets at −10.13 ppm and the broad singlet at −10.20 ppm were assigned to the two hydrides that bridge the ruthenium and aluminum centers. The appearance of a single broad resonance for the terminal aluminohydride protons indicates that there may be a rapid exchange process in solution which scrambles H3 and H4 or that $RuH(AlH_4)(P^2P_3{}^{tBu})$ (**7**) may be a monomer in solution analogous to the structure observed for $RuH(BH_4)(P^2P_3{}^{tBu})$ (**6**; Figure 2) which then crystallizes to a dimer in the solid state. We have not attempted to establish conclusively whether $RuH(AlH_4)(P^2P_3{}^{tBu})$ (**7**) exists as a dimer or a monomeric species in solution, or an equilibrium between the two.

While stable for periods of time up to a couple of hours, $RuH(AlH_4)(P^2P_3{}^{tBu})$ (**7**) decomposes upon extended (overnight) exposure to a nitrogen atmosphere, both in solution or in the solid state, with one of the multiple decomposition products identified as $RuH_2(N_2)(P^2P_3{}^{tBu})$ (**1**). $RuH(AlH_4)(P^2P_3{}^{tBu})$ (**7**) is also unstable to elevated temperatures in solution; heating a benzene or toluene solution of **7** results in the formation of multiple products.

Although $RuH(AlH_4)(P^2P_3{}^{tBu})$ (**7**) decomposes in solution and in the solid state to give small amounts of $RuH_2(N_2)(P^2P_3{}^{tBu})$ (**1**), clean separation of **1** from the remaining starting material and the resulting aluminum salts was not possible. It was, however, possible to accelerate the decomposition by treatment of $RuH(AlH_4)(P^2P_3{}^{tBu})$ (**7**) with ethanol. Reaction with ethanol resulted in complete conversion of $RuH(AlH_4)(P^2P_3{}^{tBu})$ (**7**) to $RuH_2(N_2)(P^2P_3{}^{tBu})$ (**1**) but also produced aluminum salts as byproducts, which again proved difficult to remove. Two other strategies were also attempted to convert $RuH(AlH_4)(P^2P_3{}^{tBu})$ (**7**) to $RuH_2(N_2)(P^2P_3{}^{tBu})$ (**1**), through treatment with potassium *tert*-butoxide and treatment with methanol.

K[Ru(H)$_3$(P^{2}P$_3{}^{tBu}$)] (8). Treatment of $RuH(AlH_4)(P^2P_3{}^{tBu})$ (**7**) with potassium *tert*-butoxide was used in an attempt to decompose the tetrahydridoaluminate to give $RuH_2(N_2)(P^2P_3{}^{tBu})$ (**1**). The addition of excess potassium *tert*-butoxide in THF solution to a benzene solution of $RuH(AlH_4)(P^2P_3{}^{tBu})$ (**7**) and subsequent work up afforded $K[Ru(H)_3(P^2P_3{}^{tBu})]$ (**8**) as a white powder (Scheme 7). Crystals suitable for structural analysis were grown by slow evaporation of a benzene solution of **8** under N_2 (Figure 5), and selected bond lengths and angles are included in Table 4.

Scheme 7

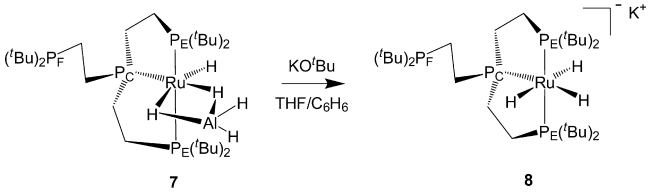

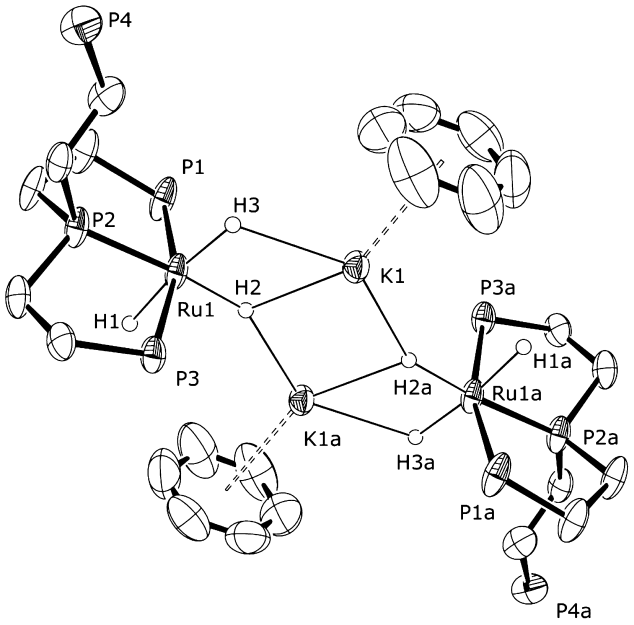

Figure 5. ORTEP plot (50% thermal ellipsoids) of $K[Ru(H)_3(P^2P_3{}^{tBu})]$ (**8**). Selected hydrogen atoms and *tert*-butyl groups have been omitted for clarity.

Table 4. Selected Bond Lengths (Å) and Bond Angles (deg) for $K[Ru(H)_3(P^2P_3{}^{tBu})]$ (8)

Ru1−H1	1.67(3)	Ru1−H2	1.74(3)
Ru1−H3	1.66(3)	Ru1−P1	2.3129(10)
Ru1−P2	2.2261(10)	Ru1−P3	2.3170(10)
Ru1−K1	3.5438(8)		
P1−Ru1−P2	84.27(4)	P1−Ru1−P3	161.92(4)
P2−Ru1−P3	82.35(4)	P1−Ru1−H1	85.5(10)
P2−Ru1−H1	86.5(11)	P3−Ru1−H1	81.6(10)
P1−Ru1−H2	94.0(10)	P2−Ru1−H2	173.3(10)
P3−Ru1−H2	97.9(10)	P1−Ru1−H3	97.3(11)
P2−Ru1−H3	100.6(12)	P3−Ru1−H3	97.1(11)
H1−Ru1−H2	86.9(15)	H1−Ru1−H3	172.5(17)
H2−Ru1−H3	86.0(16)		

dx.doi.org/10.1021/ic501895s | *Inorg. Chem.* 2014, 53, 12469−12479

$K[Ru(H)_3(P^2P_3{}^{tBu})]$ (**8**) could also be formed by the treatment of $RuH_2(N_2)(P^2P_3{}^{tBu})$ (**1**) or $RuH_2(H_2)(P^2P_3{}^{tBu})$ (**10**) with potassium hydride in THF overnight.

Trihydridoruthenate complexes are uncommon, with this being the first example with an alkyl phosphine ligand.[20] They are of particular interest as one of the only other trihydridoruthenate complexes, $K[H_3Ru(PPh_3)_3]$, has proven a versatile building block for interesting bimetallic hydride clusters.[21]

The geometry of $K[Ru(H)_3(P^2P_3{}^{tBu})]$ (**8**) is that of a distorted octahedron around ruthenium with the three phosphine donors in a meridional arrangement, and the three other coordination sites occupied by hydrides. Each metal center is part of a dimer, with interactions between two of the hydrides and two potassium ions forming a bridge between the two metal centers. The only other reported structures of trihydridoruthenates are $[K(18\text{-crown-}6)][H_3Ru(PPh_3)_3]$[20] and $[Li][Ru(\mu\text{-}H)_3(PTol_3)_3]$ which are formed through the treatment of $RuHCl(PPh_3)_3$ with 2 equiv of $KBBu_3H$. The most marked difference between the two structures is the *facial* geometric arrangement of the hydrides and phosphines of $[K(C_{12}H_{24}O_6)][H_3Ru(PPh_3)_3]$ when compared to the *meridional* binding of **8**. However, the bond lengths around ruthenium are similar to ruthenium phosphorus bond lengths of 2.338(4), 2.312(3), and 2.318(3) Å for $[K(18\text{-crown-}6)][H_3Ru(PPh_3)_3]$ compared to 2.3129(10), 2.2261(10), and 2.3170(10) Å for **8**. The ruthenium hydride bond lengths of 1.60(9), 1.59(8), and 1.70(9) Å compared to 1.67(3), 1.66(3), and 1.74(3) Å for $[K(18\text{-crown-}6)][H_3Ru(PPh_3)_3]$ and **8** respectively are also comparable. The potassium cations in both complexes are stabilized within the crystal structure by proximity to three electron rich hydrides, with distances of 2.57(8), 2.66(8), and 3.13(9) Å, compared to 2.55(4), 2.61(3), and 2.77(3) Å for $[K(18\text{-crown-}6)][H_3Ru(PPh_3)_3]$ and complex **8**, respectively. Additional stabilization is provided in $[K(18\text{-crown-}6)][H_3Ru(PPh_3)_3]$ by the common alkali metal stabilizing ligand 18-crown-6 ether where in **8** the same role is performed by a solvated benzene molecule. The *tert*-butyl groups on the coordinated terminal phosphines form steric pockets around the potassium ions and this contributes to stabilization of the cations.

The $^{31}P\{^1H\}$ NMR spectrum of $K[Ru(H)_3(P^2P_3{}^{tBu})]$ (**8**) displays the signal for the two terminal phosphines P_E as a doublet at 131.6 ppm with a $^2J_{P-P}$ = 19 Hz coupling constant to P_C. The signal for the central phosphine P_C is a broad singlet at 121.1 ppm and the pendant phosphine P_F signal appears as a doublet at 35.2 ppm with a $^3J_{P-P}$ = 31 Hz coupling constant to P_C. The ^1H NMR spectrum of $K[Ru(H)_3(P^2P_3{}^{tBu})]$ (**8**) displays three high field resonances at −9.10, −10.59, and −13.70 ppm in a ratio of 1:1:1 which are assigned to ruthenium hydrides.

$RuH_2(N_2)(P^2P_3{}^{tBu})$ (1). Treatment of $RuCl_2(P^2P_3{}^{tBu})$ with potassium graphite in THF afforded some $RuH_2(N_2)(P^2P_3{}^{tBu})$ (**1**), but again isolation from other concurrently formed byproducts proved difficult. The best method for the synthesis of **1** was by reduction of $RuCl_2(P^2P_3{}^{tBu})$ (**2**) with sodium in liquid ammonia under a N_2 atmosphere (Scheme 8).

Like all other methods used to produce **1**, a small amount of $RuH_2(H_2)(P^2P_3{}^{tBu})$ (**10**) was produced during the reaction, and this byproduct was converted to $RuH_2(N_2)(P^2P_3{}^{tBu})$ (**1**) by reducing the volume of a pentane extract under a stream of nitrogen until the yellow precipitate of $RuH_2(N_2)(P^2P_3{}^{tBu})$ (**1**) formed completely. Crystals of $RuH_2(N_2)(P^2P_3{}^{tBu})$ (**1**) suitable for structural analysis were grown by slow evaporation from a toluene solution of **1** under an atmosphere of N_2 (Figure 6), and selected bond lengths and angles are included in Table 5.

Scheme 8

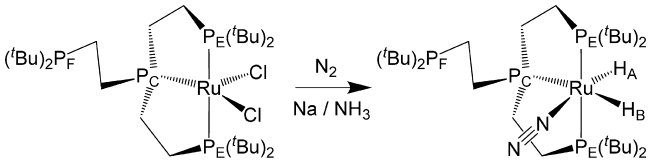

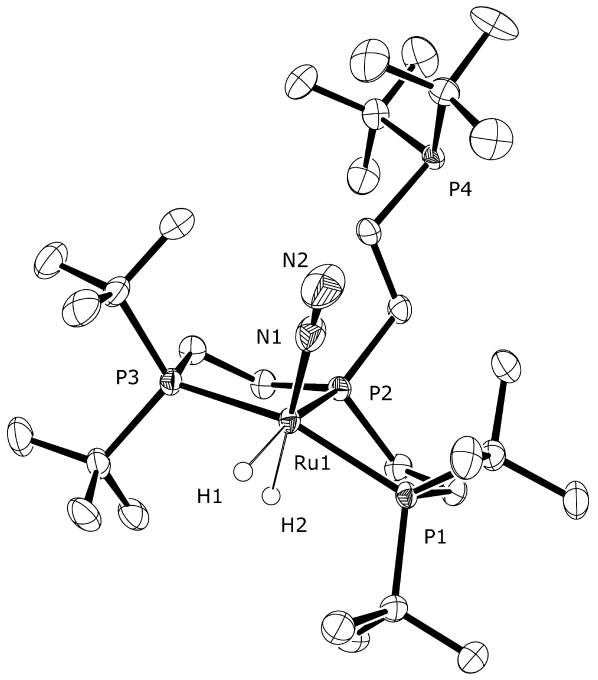

Figure 6. ORTEP plot (50% thermal ellipsoids) of $RuH_2(N_2)(P^2P_3{}^{tBu})$ (**1**), within each asymmetric unit. Selected hydrogen atoms have been omitted for clarity.

The geometry of $RuH_2(N_2)(P^2P_3{}^{tBu})$ (**1**) is that of a distorted octahedron with the three phosphine donors in a *meridional* arrangement, two hydrides in mutually *cis* coordination sites, and the dinitrogen *trans* to one of the hydrides (H2). The most closely related structure in the

Table 5. Selected Bond Lengths (Å) and Angles (deg) for $RuH_2(N_2)(P^2P_3{}^{tBu})$ (1)

Ru1−N1	1.978 (3)	Ru1−H1	1.65 (4)
Ru1−H2	1.60 (4)	Ru1−P2	2.2771 (7)
Ru1−P1	2.3281 (7)	Ru1−P3	2.3266 (7)
N1−N2	1.111 (4)		
N1−Ru1−P1	99.60 (8)	N1−Ru1−P2	111.12 (9)
N1−Ru1−P3	102.25 (8)	P1−Ru1−P3	157.99 (3)
P2−Ru1−P1	84.10 (3)	P2−Ru1−P3	85.64 (3)
N1−Ru1−H2	170.8 (13)	P2−Ru1−H2	77.5 (13)
P1−Ru1−H2	77.8 (12)	P3−Ru1−H2	81.0 (13)
N1−Ru1−H1	86.7 (14)	P2−Ru1−H1	162.2 (14)
P1−Ru1−H1	92.4 (13)	H1−Ru1−H2	84.7 (18)
P3−Ru1−H1	91.5 (13)	N2−N1−Ru1	175.2 (3)

dx.doi.org/10.1021/ic501895s | *Inorg. Chem.* 2014, 53, 12469−12479

Scheme 9

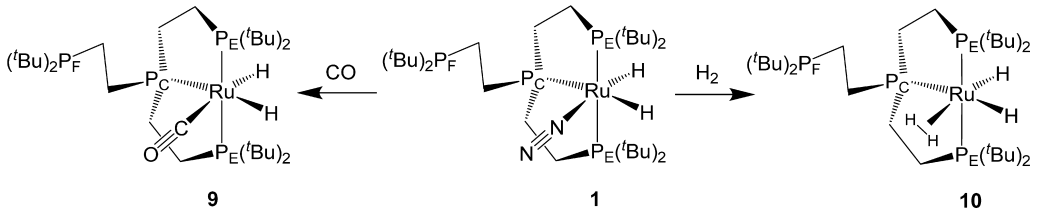

literature is that of $RuH_2(N_2)$(Cyttp) (Cyttp = C_6H_5P-$(CH_2CH_2CH_2PCy_2)_2$),[22] which shares the same geometry and ligand arrangement, with the differences being solely the nature of the phosphine ligand. The Ru−H bond lengths of the two compounds are almost identical (all between 1.60 and 1.65 Å) as are the Ru−N bonds (2.005 Å compared to 1.978 Å for **1**). The only significant difference between the two structures is the P−Ru−P bond angles, which are around 10° smaller in **1**, and this variation can be attributed to the different bite angles of the ligands.

It should be noted that the Ru−P bond lengths for the dialkyl terminal phosphines (P1 and P3) in $RuH_2(N_2)(P^2P_3{}^{tBu})$ (**1**) are significantly longer (0.051 and 0.050 Å) than the Ru−P bond for the central phosphine (P2). This pattern for the Ru−P bond lengths is consistent across the structurally characterized complexes presented: 0.162 and 0.153 Å for $RuHCl(P^2P_3{}^{tBu})$ (**3**), 0.135 and 0.136 Å for $RuH(BH_4)(P^2P_3{}^{tBu})$ (**6**), 0.078 and 0.074 Å for $RuH(AlH_4)(P^2P_3{}^{tBu})$ (**7**), as well as 0.087 and 0.091 Å for $K[Ru(H)_3(P^2P_3{}^{tBu})]$ (**8**). The pattern can be attributed to the steric bulk of the *tert*-butyl groups on the terminal phosphine donors, which can restrict their approach of the metal center.

The $^{31}P\{^1H\}$ NMR spectrum of $RuH_2(N_2)(P^2P_3{}^{tBu})$ (**1**) contains the signal for the two terminal phosphines P_E as a broad singlet at 121.7 ppm, the signal for the central phosphine P_C as a multiplet at 97.1 ppm, and the pendant phosphine P_F signal as a doublet at 35.1 ppm. The ^1H NMR resonances for the two hydrido ligands of $RuH_2(N_2)(P^2P_3{}^{tBu})$ (**1**) are located at the high field end of the spectrum. The resonance due to H_A (*trans* to the P_C ligand) appears at −7.13 ppm as a doublet of triplets of doublets corresponding to coupling to P_C, P_E, and H_B, with coupling constants of 90, 20, and 4 Hz, respectively. The large coupling to P_C indicates that H_A is *trans* to P_C, as previous work has shown coupling constants between nuclei which are *trans* in octahedral ruthenium complexes to have much higher coupling constants than those bound *cis*.[23] The second resonance corresponding to H_B (*trans* to the N_2 ligand) appears at −17.03 ppm as a triplet of doublets of doublets, corresponding to coupling to P_E, P_C, and H_A with coupling constants of 24, 21, and 4 Hz, respectively.

The infrared spectrum of $RuH_2(N_2)(P^2P_3{}^{tBu})$ (**1**) shows a sharp absorbance at 2115 cm^{-1} which is assigned to the nitrogen−nitrogen triple bond stretch $\nu(N{\equiv}N)$. The $\nu(N{\equiv}N)$ is used as a measure of the degree of activation of the N−N triple bond when bound to a metal center with frequencies generally found between the frequency for free dinitrogen at 2331 cm^{-1} and that for a diazene derivative PhN=NPh at 1442 cm^{-1}.[2a] Ruthenium nitrogen complexes typically have $\nu(N{\equiv}N)$ absorbances in the range 2029−2220 cm^{-1}, so in comparison, $RuH_2(N_2)(P^2P_3{}^{tBu})$ (**1**) has an unremarkable level of activation for a ruthenium dihydride dinitrogen complex where $\nu(N{\equiv}N)$ for two previously reported complexes of this type, $[Ru(H)_2(N_2)(PPh_3)_3]$[24] and $[Ru(H)_2(cyttp)(N_2)]$,[22] are observed at 2147 and 2100 cm^{-1}, respectively.

The N_2 ligand in $RuH_2(N_2)(P^2P_3{}^{tBu})$ (**1**) is relatively labile, and the dinitrogen ligand can be exchanged readily with $^{15}N_2$, with CO, and with H_2. Reaction of $RuH_2(N_2)(P^2P_3{}^{tBu})$ (**1**) with carbon monoxide afforded $RuH_2(CO)(P^2P_3{}^{tBu})$ (**9**) as an off-white powder, and crystals suitable for structural analysis were grown by slow evaporation of a toluene solution (Scheme 9). Characterization data and the molecular structure for $RuH_2(CO)(P^2P_3{}^{tBu})$ (**9**) are contained in the Supporting Information.

$RuH_2(^{15}N_2)(P^2P_3{}^{tBu})$ ($^{15}N_2$-1). Placing a degassed THF-d_8 solution of $RuH_2(N_2)(P^2P_3{}^{tBu})$ (**1**) under $^{15}N_2$ gas (1.5 atm) affords $RuH_2(^{15}N_2)(P^2P_3{}^{tBu})$ (**$^{15}N_2$-1**). The $^{15}N\{^1H\}$ NMR spectrum of $RuH_2(^{15}N_2)(P^2P_3{}^{tBu})$ (**$^{15}N_2$-1**) displays two broadened resonances at −44.6 ppm and −65.7 ppm corresponding to N_β and N_α, respectively, as well as a resonance at −71.5 ppm corresponding to free $^{15}N_2$ in solution. The broadness of the signals prevents the observation of any $^2J_{N-P}$ coupling, indicating a process of exchange which averages any coupling. This is also evident in the ^1H NMR spectrum of **$^{15}N_2$-1**, which displays no change in the coupling pattern for the resonances to high field assigned to the two ruthenium hydrides, when compared to those of the ^{14}N analogue $RuH_2(N_2)(P^2P_3{}^{tBu})$ (**1**). There is only a slight broadening of the H_B resonance at −17.03 ppm, preventing the observation of $^2J_{H-H}$ coupling in this resonance of **$^{15}N_2$-1**. The averaging of $^2J_{N-P}$ and $^2J_{N-H}$ couplings is evidence that the dinitrogen ligand exchanges rapidly with free N_2 in solution.

$RuH_2(H_2)(P^2P_3{}^{tBu})$ (10). Placing a degassed THF-d_8 solution of $RuH_2(N_2)(P^2P_3{}^{tBu})$ (**1**) under H_2 gas (1.5 atm) resulted in a color change from yellow to colorless and afforded a new complex which we assign as $RuH_2(H_2)(P^2P_3{}^{tBu})$ (**10**; Scheme 10).

Scheme 10

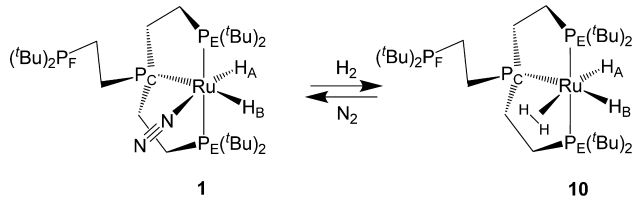

$RuH_2(H_2)(P^2P_3{}^{tBu})$ (**10**) is also produced during the synthesis of $Ru(H)_2N_2(P^2P_3{}^{tBu})$ (**1**), and the addition of hydrogen gas during the workup of **1** resulted in the formation of $RuH_2(H_2)(P^2P_3{}^{tBu})$ (**10**). ^1H NMR observation of the behavior of both $RuH_2(N_2)(P^2P_3{}^{tBu})$ (**1**) and $RuH_2(H_2)$-$(P^2P_3{}^{tBu})$ (**10**) under atmospheres of H_2 and N_2, respectively, gives some indication of the relative binding preferences for N_2 and H_2. $RuH_2(N_2)(P^2P_3{}^{tBu})$ (**1**) is converted quantitatively into

dx.doi.org/10.1021/ic501895s | *Inorg. Chem.* 2014, 53, 12469−12479

Table 6. Crystal Data Refinement Details for Complexes 1, 3B, 6, 7, and 8

compound reference	$RuH_2(N_2)(P^2P_3^{tBu})$ (**1**)	$RuHCl(P^2P_3^{tBu})$ (**3B**)	$RuH(BH_4)(P^2P_3^{tBu})$ (**6**)	$RuH(AlH_4)(P^2P_3^{tBu})$ (**7**)	$K[RuH_3(P^2P_3^{tBu})]$ (**8**)
chemical formula	$C_{30}H_{68}N_2P_4Ru$	$C_{30}H_{67}ClP_4Ru$	$C_{30}H_{71}BP_4Ru$	$C_{30}H_{71}AlP_4Ru$	$C_{36}H_{75}KP_4Ru$
formula mass	681.81	688.24	667.63	683.80	772.01
crystal system	monoclinic	monoclinic	monoclinic	triclinic	triclinic
a/Å	8.5017(6)	8.0280(6)	8.2066(3)	10.9783(3)	12.5716(8)
b/Å	21.3304(16)	22.3513(18)	22.2411(10)	13.4176(5)	12.6716(9)
c/Å	20.3462(13)	20.2652(13)	20.3594(11)	14.3526(5)	14.4181(10)
α/deg	90.00	90.00	90.00	69.2550(10)	71.966(3)
β/deg	99.815(2)	95.535(2)	96.760(3)	85.0090(10)	79.246(3)
γ/deg	90.00	90.00	90.00	69.6890(10)	83.606(3)
V/Å^3	3635.7(4)	3619.4(5)	3690.2(3)	1852.61(11)	2142.1(3)
temperature/K	150(2)	150(2)	150(2)	150(2)	150(2)
space group	$P2(1)/n$	$P2(1)/n$	$P2(1)/n$	$P\bar{1}$	$P\bar{1}$
Z	4	4	4	2	2
μ(Mo Kα) (mm^{-1})	0.628	0.701	0.615	0.637	0.634
N	23007	20013	26284	22300	26692
N_{ind}	6394	6322	6485	6486	7368
R_{int}	0.0302	0.1349	0.1140	0.0493	0.0737
final R_1 values ($I > 2\sigma(I)$)	0.0275	0.0464	0.0582	0.0253	0.0415
final $wR(F^2)$ values ($I > 2\sigma(I)$)	0.0837	0.1072	0.1085	0.0610	0.0812
final R_1 values (all data)	0.0426	0.0733	0.1188	0.0308	0.0678
final $wR(F^2)$ values (all data)	0.1098	0.1258	0.1306	0.0637	0.0931
goodness of fit on F^2	0.849	0.997	1.035	1.028	1.020

10 under a H_2 atmosphere, yet it takes multiple cycles of placing a solution of $RuH_2(H_2)(P^2P_3^{tBu})$ (**10**) under a vacuum and refilling with a N_2 atmosphere to get complete conversion back to **1**. The 16 electron $[RuH_2(P^2P_3^{tBu})]$ ruthenium dihydride core therefore has a preference for binding H_2 over N_2.

The $^{31}P\{^1H\}$ NMR spectrum of $RuH_2(H_2)(P^2P_3^{tBu})$ (**10**) displays the signal for the two terminal phosphines P_E as a doublet at 123.3 ppm with a $^2J_{P-P}$ = 8 Hz coupling constant to P_C. The signal for the central phosphine P_C is a doublet of triplets at 109.2 ppm, and the pendant phosphine P_F signal appears as a doublet at 35.9 ppm with a $^3J_{P-P}$ = 35 Hz coupling constant to P_C. The ^1H NMR spectrum of $RuH_2(H_2)(P^2P_3^{tBu})$ (**10**) displays the signals due to the alkyl groups of the ligand in the aliphatic region of the spectrum as well as a single broad resonance at −8.45 ppm in the high field region of the spectrum assigned to the ruthenium hydrides and bound dihydrogen. On lowering the temperature to 200 K, the hydride resonance broadens further and then resolves to two broad peaks at −6.94 ppm and −12.83 ppm with an integration ratio of 3:1. Where at room temperature all four of the ruthenium hydride and hydrogen ligands are in fast exchange, at low temperatures one of the ruthenium hydrides separates from the other three so that its distinct resonance can be observed, while the other hydride and the dihydrogen ligand are still in a state of rapid exchange. One can speculate that the hydride which is *cis* to the dihydrogen ligand exchanges more rapidly with the hydrogens of the H_2 ligand, and it is the hydride *trans* to the H_2 ligand whose exchange is slowed at low temperature. At least at temperatures down to 200 K, it was not possible to slow the exchange further to observe a distinct resonance for the coordinated H_2 to further characterize the dihydrogen ligand.

CONCLUSIONS

A synthetic route to the sterically hindered dihydrido dinitrogen complex $RuH_2(N_2)(P^2P_3^{tBu})$ (**1**) was developed via reduction of $RuCl_2(P^2P_3^{tBu})$ (**2**) with sodium in liquid ammonia under a nitrogen atmosphere. The complex, like other complexes containing the bulky $P^2P_3^{tBu}$ ligand, has a structure where three of the four phosphine donors are coordinated and there is one dangling pendant phosphine.

Reduction of $RuCl_2(P^2P_3^{tBu})$ (**2**) with metal hydride reducing agents (KH, $NaBH_4$, $LiAlH_4$) resulted in different hydride complexes including new dinuclear ruthenium hydride species with bridging hydrides. The formation of these usually unstable ruthenium hydride geometries can be attributed to the bulky ligands which create both a crowded yet coordinatively unsaturated Ru core to which only small donors can bind, and the bulky ligands also provide a shield which protects the metal center and the small donors once the complexes have been formed.

The dinitrogen complex $RuH_2(N_2)(P^2P_3^{tBu})$ (**1**) exhibits a moderate degree of N_2 activation, and the N_2 ligand is labile and is readily exchanged for H_2 and for CO. Complex **1** is only the second ruthenium dinitrogen dihydride to be characterized structurally.

EXPERIMENTAL SECTION

General Information. All manipulations were carried out using standard Schlenk, vacuum, and glovebox techniques under a dry atmosphere of nitrogen. Solvents were dried, distilled under nitrogen or argon using standard procedures,[25] and stored in glass ampules fitted with Youngs Teflon taps. Benzene was dried over sodium wire before distillation from sodium/benzophenone, while ethanol and methanol were distilled from diethoxymagnesium or dimethoxymagnesium, respectively. THF (inhibitor free), toluene, and pentane were dried and deoxygenated using a Pure Solv 400-4-MD (Innovative Technology) solvent purification system. Deuterated solvents THF-d_8, toluene-d_8, and benzene-d_6 were dried and distilled from sodium/benzophenone and were vacuum distilled immediately prior to use. $RuCl_2(P^2P_3^{tBu})$ (**2**) was prepared by literature methods.[11] $LiAlH_4$ was purchased from Aldrich, and a concentrated solution in THF produced by Soxhlet extraction. Air sensitive NMR samples were prepared in an argon- or nitrogen-filled glovebox or on a high vacuum line by vacuum transfer of solvent into an NMR tube fitted with a concentric Teflon valve. ^1H, ^{15}N, $^{13}C\{^1H\}$, and $^{31}P\{^1H\}$ spectra were recorded on Bruker

dx.doi.org/10.1021/ic501895s | Inorg. Chem. 2014, 53, 12469−12479

DPX300, Avance III 400, Avance III 500, or Avance III 600 NMR spectrometers operating at 300, 400, 500, and 600 MHz for ^{1}H; 100.61 MHz for ^{13}C{^{1}H}; 40.6 MHz for ^{15}N and ^{15}N{^{1}H}; and 121.49, 161.98, and 242.95 MHz for ^{31}P{^{1}H}, respectively. All NMR spectra were recorded at 298 K, unless stated otherwise. ^{1}H and ^{13}C{^{1}H} NMR spectra were referenced to solvent resonances. ^{31}P{^{1}H} NMR spectra were referenced to external neat trimethyl phosphite at 140.85 ppm. ^{15}N and ^{15}N{^{1}H} spectra were referenced to external neat nitromethane at 0 ppm. Microanalyses were carried out at the Campbell Microanalytical Laboratory, University of Otago, New Zealand. Details of the X-ray analyses are given in Table 6.

Synthesis of RuHCl($P^2P_3^{tBu}$) (3). A suspension of potassium hydride (37 mg, 0.92 mmol) and $RuCl_2(P^2P_3^{tBu})$ (**2**; 57 mg, 0.079 mmol) in THF (20 mL) was stirred at room temperature overnight. The color of the brown suspension changed to orange, and the solution was filtered through Celite. The filtrate was evaporated to dryness under reduced pressure, and the resultant residue was taken up in benzene (5 mL) and filtered. The benzene solution was heated at 60 °C for 6 h, and volatiles were removed under reduced pressure to give $RuHCl(P^2P_3^{tBu})$ (**3**; 36 mg, 0.052 mmol, 66% from $RuCl_2(P^2P_3^{tBu})$) as an orange crystalline powder. Anal. Found: C, 52.06; H, 9.95. $C_{30}H_{67}ClRuP_4$ (MW 688.28) requires C, 52.35; H, 9.81.

Kinetic Isomer **3A**, ^{31}P{^{1}H} NMR (162 MHz, benzene-d_6): δ 115.9 (1P, dt, $^{3}J_{PC-PF}$ = 21 Hz, $^{2}J_{PC-PE}$ = 17 Hz, $\mathbf{P_C}$); 82.3 (2P, d, $^{2}J_{PE-PC}$ = 17 Hz, $\mathbf{P_E}$); 33.9 (1P, d, $^{3}J_{PF-PC}$ = 31 Hz, $\mathbf{P_F}$). ^{1}H NMR (400 MHz, benzene-d_6): δ 2.25 (2H, m, C$\mathbf{H_2}$); 2.00 (2H, m, C$\mathbf{H_2}$); 1.83 (2H, m, C$\mathbf{H_2}$); 1.49 (2H, m, C$\mathbf{H_2}$); 1.44 (18H, t, $^{3}J_{H-P}$ = 6 Hz, C$\mathbf{H_3}$); 1.39 (2H, m, C$\mathbf{H_2}$); 1.32 (18H, t, $^{3}J_{H-P}$ = 6 Hz, C$\mathbf{H_3}$); 1.10 (18H, d, $^{3}J_{H-P}$ = 11 Hz, C$\mathbf{H_3}$); 0.76 (2H, m, C$\mathbf{H_2}$); −30.61 (1H, dt, $^{2}J_{H-P}$ = 42 Hz, $^{2}J_{H-P}$ = 18 Hz, Ru**H**).

Thermodynamic Isomer **3B**, ^{31}P{^{1}H} NMR (162 MHz, benzene-d_6): δ 120.8 (1P, dt, $^{3}J_{PC-PF}$ = 30 Hz, $^{2}J_{PC-PE}$ = 14 Hz, $\mathbf{P_C}$); 86.4 (2P, d, $^{2}J_{PE-PC}$ = 14 Hz, $\mathbf{P_E}$); 33.7 (1P, d, $^{3}J_{PF-PC}$ = 30 Hz, $\mathbf{P_F}$). ^{1}H NMR (500 MHz, benzene-d_6): δ 2.25 (2H, m, C$\mathbf{H_2}$); 2.00 (2H, m, C$\mathbf{H_2}$); 1.83 (2H, m, C$\mathbf{H_2}$); 1.49 (2H, m, C$\mathbf{H_2}$); 1.44 (18H, t, $^{3}J_{H-P}$ = 6 Hz, C$\mathbf{H_3}$); 1.39 (2H, m, C$\mathbf{H_2}$); 1.32 (18H, t, $^{3}J_{H-P}$ = 6 Hz, C$\mathbf{H_3}$); 1.10 (18H, d, $^{3}J_{H-P}$ = 11 Hz, C$\mathbf{H_3}$); 0.76 (2H, m, C$\mathbf{H_2}$); −30.47 (1H, dt, $^{2}J_{H-P}$ = 43 Hz, $^{2}J_{H-P}$ = 19 Hz, Ru**H**). ^{13}C{^{1}H} NMR (100.6 MHz, benzene-d_6): δ 37.3 (t, $^{1}J_{C-P}$ = 4 Hz, $\mathbf{C}(CH_3)_3$); 36.3 (t, $^{1}J_{C-P}$ = 6 Hz, $\mathbf{C}(CH_3)_3$); 31.6 (d, $^{1}J_{C-P}$ = 24 Hz, $\mathbf{C}(CH_3)_3$); 30.1 (t, $^{2}J_{C-P}$ = 3 Hz, C$\mathbf{C}H_3)_3$); 30.0 (t, $^{2}J_{C-P}$ = 3 Hz, C$\mathbf{C}H_3)_3$); 29.9 (m, $\mathbf{C}H_2$); 29.8 (d, $^{2}J_{C-P}$ = 14 Hz, C$\mathbf{C}H_3)_3$); 28.6 (dd, $^{1}J_{C-P}$ = 25 Hz, $^{2}J_{C-P}$ = 17 Hz, $\mathbf{C}H_2$); 22.1 (dt, $^{1}J_{C-P}$ = 11 Hz, $^{2}J_{C-P}$ = 9 Hz, $\mathbf{C}H_2$); 16.3 (dd, $^{1}J_{C-P}$ = 28 Hz, $^{2}J_{C-P}$ = 7 Hz, $\mathbf{C}H_2$). Crystals of **3B** suitable for structural analysis were grown by evaporation of a 1:1 THF/toluene solution.

Synthesis of RuHCl(CO)($P^2P_3^{tBu}$) (4). A solution of RuHCl($P^2P_3^{tBu}$) (**3**) (48 mg, 0.070 mmol) in benzene (5 mL) was degassed by three freeze−pump−thaw cycles before addition of an atmosphere of carbon monoxide. The color of the solution changed from deep red to colorless. Volatiles were removed under reduced pressure to afford RuHCl(CO)($P^2P_3^{tBu}$) (**4**; 37 mg, 0.052 mmol, 74% by RuHCl($P^2P_3^{tBu}$)) as a white solid. Anal. found: C, 52.27; H, 9.54. $RuClOC_{31}H_{67}P_4$ (MW 716.29) requires C, 51.98; H, 9.43. Crystals of RuHCl(CO)($P^2P_3^{tBu}$) (**4**) suitable for structural analysis were grown by slow evaporation of a toluene solution. ^{31}P{^{1}H} NMR (243 MHz, benzene-d_6): δ 113.8 (1P, dt, $^{3}J_{P-P}$ = 33 Hz, $^{3}J_{P-P}$ = 7 Hz, $\mathbf{P_C}$); 99.6 (2P, d, $^{3}J_{P-P}$ = 7 Hz, $\mathbf{P_E}$); 34.0 (1P, d, $^{3}J_{P-P}$ = 33 Hz, $\mathbf{P_F}$). ^{1}H NMR (600 MHz, benzene-d_6): δ 1.90 (2H, m, C$\mathbf{H_2}$); 1.62 (4H, m, C$\mathbf{H_2}$); 1.50 (18H, t, $^{3}J_{H-P}$ = 6 Hz, C$\mathbf{H_3}$); 1.45 (2H, m, C$\mathbf{H_2}$); 1.38 (18H, t, $^{3}J_{H-P}$ = 6 Hz, C$\mathbf{H_3}$); 1.32 (4H, m, C$\mathbf{H_2}$); 1.11 (18H, d, $^{3}J_{H-P}$ = 11 Hz, C$\mathbf{H_3}$); −7.39 (1H, dt, $^{2}J_{H-P}$ = 25 Hz, $^{2}J_{H-P}$ = 25 Hz, Ru**H**). IR (fluorolube): ν 1968 s (C≡O), 1875 s (Ru−H) cm^{-1}.

Synthesis of RuHCl(N_2)($P^2P_3^{tBu}$) (5). A solution of RuHCl($P^2P_3^{tBu}$) (**1**; 21 mg, 31 μmol) in a 1:2 mixture of THF/hexane was allowed to evaporate through a septum over a period of 4 weeks under an atmosphere of nitrogen to afford red crystals (6.5 mg, 9.1 μmol, 29% by RuHCl($P^2P_3^{tBu}$)). The crystals were suitable for structural analysis. RuHCl(N_2)($P^2P_3^{tBu}$) (**5**) is unstable when dried or when left for prolonged periods in benzene and THF solutions, preventing NMR characterization or microanalysis.

Synthesis of RuH(BH_4)($P^2P_3^{tBu}$) (6). $RuCl_2(P^2P_3^{tBu})$ (**2**; 50 mg, 0.069 mmol) and $NaBH_4$ (50 mg, 1.3 mmol) were stirred in methanol (15 mL) for 16 h, resulting in the formation of a light yellow precipitate. The product, RuH(BH_4)($P^2P_3^{tBu}$) (**6**; 30 mg, 0.045 mmol, 65% by $RuCl_2(P^2P_3^{tBu})$), was collected by filtration. Anal. Found: C, 53.63; H, 10.43. $RuBP_4C_{30}H_{71}$ (MW 667.67) requires C, 53.97; H, 10.72. Crystals suitable for structural analysis were grown by evaporation of a toluene solution.

^{31}P{^{1}H} NMR (162 MHz, benzene-d_6): δ 118.5 (1P, dt, $^{3}J_{PC-PF}$ = 37 Hz, $^{3}J_{PC-PE}$ = 11 Hz, $\mathbf{P_C}$); 97.7 (2P, d, $^{3}J_{PE-PC}$ = 11 Hz, $\mathbf{P_E}$); 35.5 (1P, d, $^{3}J_{PF-PC}$ = 37 Hz, $\mathbf{P_F}$). ^{1}H NMR (400 MHz, benzene-d_6): δ 5.49 (2H, s br, B$\mathbf{H_2}$); 2.05−1.85 (4H, m, C$\mathbf{H_2}$); 1.80 (2H, m, C$\mathbf{H_2}$); 1.58−1.38 (2H, m, C$\mathbf{H_2}$); 1.45 (18H, t, $^{3}J_{H-P}$ = 6 Hz, C$\mathbf{H_3}$); 1.38−1.23 (2H, m, C$\mathbf{H_2}$); 1.28 (18H, t, $^{3}J_{H-P}$ = 6 Hz, C$\mathbf{H_3}$); 1.2−1.15 (2H, m, C$\mathbf{H_2}$); 1.12 (18H, d, $^{3}J_{H-P}$ = 11 Hz, C$\mathbf{H_3}$); −6.26 (2H, s br, Ru**H**B); −19.18 (1H, dt, $^{2}J_{H-P}$ = 36 Hz, $^{2}J_{H-P}$ = 20 Hz, Ru**H**).

Synthesis of RuH(AlH_4)($P^2P_3^{tBu}$) (7). A solution of $LiAlH_4$ in THF (∼1.5 M) was added dropwise to a stirred solution of $RuCl_2(P^2P_3^{tBu})$ (**2**; 106 mg, 0.147 mmol) in THF (10 mL) until a color change from brown to colorless was observed. Volatiles were removed under reduced pressure and the white residue extracted with benzene (10 mL). The benzene solution was filtered through Celite and the volatiles removed to afford RuH(AlH_4)($P^2P_3^{tBu}$) (**7**) (80.0 mg, 0.117 mmol, 80% by $RuCl_2(P^2P_3^{tBu})$). RuH(AlH_4)($P^2P_3^{tBu}$) (**7**) was unstable once isolated. In both the solution and solid state forms, it would degrade after a few days, and the instability prevented effective microanalysis. Crystals suitable for structural analysis were grown from a concentrated benzene-d_6 solution.

^{31}P{^{1}H} NMR (121.5 MHz, THF-d_8): δ 113.5 (2P, d, $^{2}J_{P-P}$ = 16 Hz, $\mathbf{P_E}$); 111.7 (1P, dt, $^{3}J_{P-P}$ = 32 Hz, $^{2}J_{P-P}$ = 16 Hz, $\mathbf{P_C}$); 35.1 (1P, d, $^{3}J_{P-P}$ = 32 Hz, $\mathbf{P_F}$). ^{1}H NMR (400 MHz, THF-d_8): δ 2.81 (2H, s br, Ru(μ_2-H$_2$Al$\mathbf{H_2}$)); 2.05−1.55 (6H, m, C$\mathbf{H_2}$); 1.46 (2H, m, C$\mathbf{H_2}$); 1.26 (36H, m, C$\mathbf{H_3}$); 1.17 (2H, m, C$\mathbf{H_2}$); 1.08 (2H, m, C$\mathbf{H_2}$); 1.05 (18H, d, $^{3}J_{H-P}$ = 10.5 Hz, C$\mathbf{H_3}$); −10.13 (1H, dt, $^{2}J_{H-P}$ = 53 Hz, $^{2}J_{H-P}$ = 14.1 Hz, Ru(μ_2-$\mathbf{H}_2$AlH$_2$)); −10.20 (1H, s br, Ru(μ_2-$\mathbf{H}_2$AlH$_2$)); −13.54 (1H, dtd, $^{2}J_{H-P}$ = 22 Hz, $^{2}J_{H-P}$ = 22 Hz, $^{2}J_{H-H}$ = 6.6 Hz, Ru**H**). ^{13}C{^{1}H} NMR (100.6 MHz, THF-d_8): δ 35.5 (t, $^{1}J_{C-P}$ = 9 Hz, $\mathbf{C}(CH_3)_3$); 34.7 (t, $^{1}J_{C-P}$ = 3 Hz, $\mathbf{C}(CH_3)_3$); 33.7 (dd, $^{1}J_{C-P}$ = 26 Hz, $^{2}J_{C-P}$ = 11 Hz, $\mathbf{C}H_2$); 31.6 (d, $^{1}J_{C-P}$ = 24 Hz, $\mathbf{C}(CH_3)_3$); 30.8 (t, $^{2}J_{C-P}$ = 3 Hz, C$\mathbf{C}H_3)_3$); 30.1 (t, $^{2}J_{C-P}$ = 2 Hz, C$\mathbf{C}H_3)_3$); 29.9−29.0 (m, $\mathbf{C}H_2$), 29.5 (d, $^{2}J_{C-P}$ = 14 Hz, C$\mathbf{C}H_3)_3$); 26.1−25.5 (m, $\mathbf{C}H_2$); 17.0 (d, $^{1}J_{C-P}$ = 26 Hz, $\mathbf{C}H_2$).

Synthesis of K[$RuH_3(P^2P_3^{tBu})$] (8). A concentrated solution of $LiAlH_4$ in THF was added dropwise to a solution of $RuCl_2(P^2P_3^{tBu})$ (**2**; 106 mg, 0.147 mmol) in THF (10 mL) until a color change from brown to colorless was observed. Volatiles were removed under reduced pressure, and the white residue was extracted with benzene (10 mL). The benzene solution was filtered through Celite and all volatiles removed under reduced pressure. Potassium *tert*-butoxide (34 mg, 0.30 mmol) in THF (10 mL) was added, resulting in a light yellow solution; volatiles were again removed under reduced pressure and the residue stirred with toluene (5 mL), which was then filtered through Celite. The solution was evaporated to afford K[$Ru(H)_3(P^2P_3^{tBu})$] (**8**; 53 mg, 0.076 mmol, 52%) as a very pale yellow solid. K[$Ru(H)_3(P^2P_3^{tBu})$] (**8**) was unstable to the drying procedure for microanalysis and decomposed under a vacuum. Crystals suitable for structural analysis were grown by slow evaporation of a benzene solution of **8** under N_2. ^{31}P{^{1}H} NMR (162 MHz, benzene-d_6): δ 131.6 (2P, d, $^{2}J_{P-P}$ = 19 Hz, $\mathbf{P_E}$); 121.1 (1P, s br, $\mathbf{P_C}$); (1P, d, $^{2}J_{P-P}$ = 31 Hz, $\mathbf{P_F}$). ^{1}H NMR (400 MHz, benzene-d_6): δ 2.23 (2H, m, C$\mathbf{H_2}$); 2.10 (2H, m, C$\mathbf{H_2}$); 1.84 (2H, m, C$\mathbf{H_2}$); 1.74 (2H, m, C$\mathbf{H_2}$); 1.60 (2H, m, C$\mathbf{H_2}$); 1.45 (36H, m, C$\mathbf{H_3}$); 1.17 (2H, m, C$\mathbf{H_2}$); 1.24 (18H, d, $^{3}J_{H-P}$ = 10.4 Hz, C$\mathbf{H_3}$); −9.10 (1H, m, Ru**H**); −10.59 (1H, m, Ru**H**); −13.70 (1H, m, Ru**H**).

Synthesis of $RuH_2(N_2)(P^2P_3^{tBu})$ (1). $RuCl_2(P^2P_3^{tBu})$ (**2**; 263 mg, 0.364 mmol) and freshly cut sodium metal (242 mg, 10.5 mmol) were stirred in refluxing liquid ammonia for 2 h. The liquid ammonia was

dx.doi.org/10.1021/ic501895s | Inorg. Chem. 2014, 53, 12469−12479

allowed to boil off, and the remaining contents of the flask were dried *in vacuo* for 30 min. Pentane (50 mL) was added and the solution stirred for 15 min before filtration through Celite. The solution volume was reduced to approximately 4 mL under a stream of nitrogen, resulting in the formation of a yellow precipitate. The solid was collected by filtration and dried on a small frit to afford $RuH_2(N_2)(P^2P_3^{tBu})$ (**1**; 119 mg, 0.175 mmol, 48% yield from $RuCl_2(P^2P_3^{tBu})$). Anal. Found: C, 53.07; H, 10.35, N, 3.09. $RuN_2C_{30}H_{68}P_4$ (MW 681.85) requires C, 52.85; H, 10.05; N, 4.11. Elemental analysis performed on the crystalline product suggests some loss of weakly bound dinitrogen ligand upon application of a vacuum during the analytical procedure. Crystals of $RuH_2(N_2)(P^2P_3^{tBu})$ (**1**) suitable for structural analysis were grown by slow evaporation from a toluene solution of **1** under an atmosphere of N_2. $^{31}P\{^1H\}$ NMR (162 MHz, THF-d_8): δ 121.7 (2P, s br, $\mathbf{P_E}$); 97.1 (1P, m, $\mathbf{P_C}$); 35.1 (1P, d, $^3J_{P-P}$ = 34 Hz, $\mathbf{P_F}$). $^1H\{^{31}P\}$ NMR (400 MHz, THF-d_8): δ 2.05−1.85 (4H, m, CH_2); 1.77 (4H, m, CH_2); 1.48 (4H, m, CH_2); 1.33 (18H, s, CH_3); 1.25 (18H, s, CH_3); 1.09 (18H, s, CH_3); −7.13 (1H, d, $^2J_{H-H}$ = 4 Hz, Ru$\mathbf{H_A}$); −17.03 (1H, d, $^2J_{H-H}$ = 4 Hz, Ru$\mathbf{H_B}$). ^1H NMR (400 MHz, THF-d_8, high field only): δ −7.13 (1H, dtd, $^2J_{H-P}$ = 90 Hz, $^2J_{H-P}$ = 20 Hz, $^2J_{H-H}$ = 4 Hz, RuH); −17.03 (1H, tdd, $^2J_{H-P}$ = 24 Hz, $^2J_{H-P}$ = 21 Hz, $^2J_{H-H}$ = 4 Hz, RuH). IR (fluorolube): ν 2115 s (N≡N), 1798 s br (Ru−H) cm^{-1}.

Synthesis of $RuH_2(^{15}N_2)(P^2P_3^{tBu})$ ($^{15}N_2$-1). $RuH_2(N_2)(P^2P_3^{tBu})$ (**1**; 40 mg, 0.059 mmol) was dissolved in THF-d_6 (0.5 mL) in an NMR tube fitted with a concentric Teflon valve under dinitrogen. The solution was degassed with two freeze−pump−thaw cycles then frozen in liquid nitrogen and evacuated for a third time before the introduction of $^{15}N_2$ to the NMR tube headspace. The solution was thawed and allowed to warm to room temperature, affording a solution of $RuH_2(^{15}N_2)(P^2P_3^{tBu})$ (**$^{15}N_2$-1**) suitable for NMR analysis. $^{15}N\{^1H\}$ NMR (40.6 MHz, THF-d_8): δ −44.6 (1N, s br, N_β); −65.7 (1N, s br, N_α). ^1H NMR (400 MHz, THF-d_8, high field only): δ −7.13 (1H, dtd, $^2J_{H-P}$ = 90 Hz, $^2J_{H-P}$ = 20 Hz, $^2J_{H-H}$ = 4 Hz, RuH); −17.03 (1H, td br, $^2J_{H-P}$ = 23 Hz, $^2J_{H-P}$ = 22 Hz).

Synthesis of $RuH_2(CO)(P^2P_3^{tBu})$ (9). $RuH_2(N_2)(P^2P_3^{tBu})$ (**1**; 40 mg, 0.059 mmol) was dissolved in toluene (3 mL) and degassed through a series of freeze pump thaw cycles and left under a vacuum. Carbon monoxide (1.2 atm.) was introduced to the flask and the solution stirred for 10 min. Volatiles were then removed under reduced pressure to give an off-white powder, which was recrystallized from pentane to give $RuH_2(CO)(P^2P_3^{tBu})$ (**9**; 26 mg, 0.038 mmol, 65% yield) as very pale yellow crystals. Anal. Found: C, 54.47; H, 10.16. $RuOC_{31}H_{68}P_4$ (MW 681.85) requires C, 54.61; H, 10.05. Crystals suitable for structural analysis were grown by slow evaporation from a toluene solution of **9** under an atmosphere of N_2. $^{31}P\{^1H\}$ NMR (121.5 MHz, toluene-d_8): δ 122.3 (2P, d, $^2J_{P-P}$ = 5 Hz, P_E); 98.8 (1P, dt, $^3J_{P-P}$ = 38 Hz, $^3J_{P-P}$ = 5 Hz, P_C); 30.8 (1P, d, $^3J_{P-P}$ = 38 Hz, P_F). ^1H NMR (300 MHz, toluene-d_8): δ 1.90−1.70 (4H, m, CH_2); 1.63−1.53 (2H, m, CH_2); 1.50−1.32 (6H, m, CH_2); 1.29 (18H, t, J_{H-P} = 6 Hz, CH_3); 1.25 (18H, t, J_{H-P} = 6 Hz, CH_3); 1.15 (18H, d, $^2J_{H-P}$ = 10 Hz, CH_3); −7.68 (1H, dtd, $^2J_{H-P}$ = 83 Hz, $^2J_{H-P}$ = 19 Hz, $^2J_{H-H}$ = 2 Hz, Ru$\mathbf{H_A}$); −11.38 (1H, dt br, $^2J_{H-P}$ = 20 Hz, $^2J_{H-P}$ = 19 Hz, Ru$\mathbf{H_B}$). IR (fluorolube): ν 1959 s (C≡O) cm^{-1}.

Synthesis of $RuH_2(H_2)(P^2P_3^{tBu})$ (10). $RuH_2(N_2)(P^2P_3^{tBu})$ (**1**; 35 mg, 0.051 mmol) was dissolved in THF-d_6 (0.5 mL) in an NMR tube fitted with a concentric Teflon valve under dinitrogen. The solution was degassed with two freeze−pump−thaw cycles then frozen in liquid nitrogen and evacuated for a third time before the introduction of 1.3 atm of H_2 gas to the NMR tube headspace. The solution was thawed and the NMR tube shaken, resulting in a color change from yellow to colorless giving a pure solution of $RuH_2(H_2)(P^2P_3^{tBu})$ (**10**). $RuH_2(H_2)(P^2P_3^{tBu})$ (**10**) needed to be kept under a hydrogen atmosphere to retain complete purity, and this prevented elemental analysis. $^{31}P\{^1H\}$ NMR (243 MHz, THF-d_8): δ 123.3 (2P, d, $^3J_{P-P}$ = 8 Hz, $\mathbf{P_E}$); 109.2 (1P, dt, $^3J_{P-P}$ = 35 Hz, $^3J_{P-P}$ = 8 Hz, $\mathbf{P_C}$); 35.9 (1P, d, $^3J_{P-P}$ = 35 Hz, $\mathbf{P_F}$). ^1H NMR (300 MHz, THF-d_8): δ 2.1−1.7 (8H, m, CH_2); 1.6−1.45 (4H, m, CH_2); 1.45−1.25 (18H, m, CH_3); 1.25−1.0 (36H, m, CH_3); −8.45 (4H, s br, Ru$\mathbf{H_2}$($\mathbf{H_2}$)). ^1H NMR (600 MHz, 200 K, THF-d_8, high field only): δ −6.94 (3H, s br, Ru($\mathbf{H_2}$)**H**); −12.83 (1H, s br, Ru**H**).

■ ASSOCIATED CONTENT

Supporting Information

A CIF file with crystallographic data for compounds **1**, **3B**, **4**, **5**, **6**, **7**, **8**, and **10**. Details of the structures and crystallographic parameters for compounds **4**, **5**, and **9**. This material is available free of charge via the Internet at http://pubs.acs.org.

■ AUTHOR INFORMATION

Corresponding Author

*E-mail: l.field@unsw.edu.au. Phone: +61 2 9385 2700. Fax: +61 2 9385 8008.

Notes

The authors declare no competing financial interest.

■ ACKNOWLEDGMENTS

The authors wish to thank Dr. Hsiu Lin Li for technical assistance, proof reading, and discussions. The authors also thank the Australian Research Council for financial support, and R.G.-W. thanks the Australian Government and the University of New South Wales for postgraduate scholarships. NMR spectra and mass spectra were obtained through the Mark Wainwright Analytical Centre at the University of New South Wales. Subsidized access to these facilities is gratefully acknowledged.

■ REFERENCES

(1) Allen, A. D.; Senoff, C. W. *Chem. Commun.* **1965**, 621−2.
(2) (a) Fryzuk, M. D.; Johnson, S. A. *Coord. Chem. Rev.* **2000**, *200−202*, 379−409. (b) Hidai, M. *Coord. Chem. Rev.* **1999**, *185−186*, 99−108. (c) MacKay, B. A.; Fryzuk, M. D. *Chem. Rev.* **2004**, *104*, 385−401.
(3) (a) Laplaza, C. E.; Cummins, C. C. *Science* **1995**, *268*, 861−3. (b) Yandulov, D. V.; Schrock, R. R. *J. Am. Chem. Soc.* **2002**, *124*, 6252−6253. (c) Betley, T. A.; Peters, J. C. *J. Am. Chem. Soc.* **2004**, *126*, 6252−6254. (d) Fryzuk, M. D.; Johnson, S. A.; Patrick, B. O.; Albinati, A.; Mason, S. A.; Koetzle, T. F. *J. Am. Chem. Soc.* **2001**, *123*, 3960−3973. (e) Arashiba, K.; Miyake, Y.; Nishibayashi, Y. *Nat. Chem.* **2011**, *3*, 120−125. (f) Creutz, S. E.; Peters, J. C. *J. Am. Chem. Soc.* **2014**, *136*, 1105−1115. (g) Anderson, J. S.; Rittle, J.; Peters, J. C. *Nature* **2013**, *501*, 84−87.
(4) (a) Dance, I. *Biochemistry* **2006**, *45*, 6328−40. (b) Thorneley, R. N. F.; Eady, R. R.; Lowe, D. J. *Nature* **1978**, *272*, 557−8. (c) Dance, I. *J. Am. Chem. Soc.* **2005**, *127*, 10925−10942.
(5) (a) Bianchini, C.; Laschi, F.; Peruzzini, M.; Zanello, P. *Gazz. Chim. Ital.* **1994**, *124*, 271−5. (b) King, R. B.; Kapoor, R. N.; Saran, M. S.; Kapoor, P. N. *Inorg. Chem.* **1971**, *10*, 1851−60. (c) Stoppioni, P.; Mani, F.; Sacconi, L. *Inorg. Chim. Acta* **1974**, *11*, 227−30.
(6) (a) Field, L. D.; Messerle, B. A.; Smernik, R. J.; Hambley, T. W.; Turner, P. *Inorg. Chem.* **1997**, *36*, 2884−2892. (b) Field, L. D.; Messerle, B. A.; Smernik, R. J. *Inorg. Chem.* **1997**, *36*, 5984−5990.
(7) Field, L. D.; Guest, R. W.; Vuong, K. Q.; Dalgarno, S. J.; Jensen, P. *Inorg. Chem.* **2009**, *48*, 2246−2253.
(8) Gilbert-Wilson, R.; Field, L. D.; Bhadbhade, M. M. *Inorg. Chem.* **2012**, *51*, 3239−46.
(9) Jia, G.; Drouin, S. D.; Jessop, P. G.; Lough, A. J.; Morris, R. H. *Organometallics* **1993**, *12*, 906−16.
(10) (a) Osman, R.; Pattison, D. I.; Perutz, R. N.; Bianchini, C.; Casares, J. A.; Peruzzini, M. *J. Am. Chem. Soc.* **1997**, *119*, 8459−8473. (b) Gilbert-Wilson, R.; Field, L. D.; Colbran, S. B.; Bhadbhade, M. M. *Inorg. Chem.* **2013**, *52*, 3043−3053.
(11) Gilbert-Wilson, R.; Field, L. D.; Bhadbhade, M. M. *Inorg. Chem.* **2012**, *51*, 3239−3246.

(12) Addison, A. W.; Rao, T. N.; Reedijk, J.; van Rijn, J.; Verschoor, G. C. *J. Chem. Soc., Dalton Trans.* **1984**, 1349−1356.
(13) Abdur-Rashid, K.; Lough, A. J.; Morris, R. H. *Organometallics* **2001**, *20*, 1047−1049.
(14) Hadzovic, A.; Lough, A. J.; Morris, R. H.; Pringle, P. G.; Zambrano-Williams, D. E. *Inorg. Chim. Acta* **2006**, *359*, 2864−2869.
(15) Jung, S.; Brandt, C. D.; Wolf, J.; Werner, H. *Dalton Trans.* **2004**, 375−383.
(16) Statler, J. A.; Wilkinson, G.; Thornton-Pett, M.; Hursthouse, M. B. *J. Chem. Soc., Dalton Trans.* **1984**, 1731−1738.
(17) Lin, W.; Wilson, S. R.; Girolami, G. S. *Organometallics* **1997**, *16*, 2987−2994.
(18) Etkin, N.; Hoskin, A. J.; Stephan, D. W. *J. Am. Chem. Soc.* **1997**, *119*, 11420−11424.
(19) Girolami, G. S.; Wilkinson, G.; Thornton-Pett, M.; Hursthouse, M. B. *J. Am. Chem. Soc.* **1983**, *105*, 6752−6753.
(20) Chan, A. S. C.; Shieh, H.-S. *J. Chem. Soc., Chem. Commun.* **1985**, 1379−1380.
(21) (a) Plois, M.; Wolf, R.; Hujo, W.; Grimme, S. *Eur. J. Inorg. Chem.* **2013**, *2013*, 3039−3048. (b) Plois, M.; Hujo, W.; Grimme, S.; Schwickert, C.; Bill, E.; de Bruin, B.; Pöttgen, R.; Wolf, R. *Angew. Chem., Int. Ed.* **2013**, *52*, 1314−1318. (c) Poulton, J. T.; Folting, K.; Caulton, K. G. *Organometallics* **1992**, *11*, 1364−1372. (d) Alvarez, D.; Lundquist, E. G.; Ziller, J. W.; Evans, W. J.; Caulton, K. G. *J. Am. Chem. Soc.* **1989**, *111*, 8392−8398.
(22) Jia, G.; Meek, D. W.; Gallucci, J. C. *Inorg. Chem.* **1991**, *30*, 403−410.
(23) Bampos, N.; Field, L. D.; Messerle, B. A. *Organometallics* **1993**, *12*, 2529−2535.
(24) Knoth, W. H. *J. Am. Chem. Soc.* **1968**, *90*, 7172−7172.
(25) Perrin, D. D. A.; Armarego, W. L. F. *Purification of Laboratory Chemicals*, 3rd ed.; Pergamon Press: Oxford, 1993.